JOURNAL OF CATALYSIS 140, 53–70 (1993)

Non-Faradaic Electrochemical Modification of Catalytic Activity

VII. The Case of Methane Oxidation on Platinum

P. TSIAKARAS AND C. G. VAYENAS

Institute of Chemical Engineering & High Temperature Chemical Processes, University of Patras, Patras GR-26110, Greece

Received May 18, 1992; revised September 11, 1992

It was found that the catalytic activity of Pt for the oxidation of CH_4 can be increased reversibly by up to 7000% by depositing polycrystalline Pt films on Y_2O_3-doped ZrO_2, an O^{2-} conductor, and by polarizing the Pt–solid electrolyte interface. The catalytic rate is enhanced, to a different extent, both by supplying and by removing O^{2-} to or from the Pt catalyst through the gas-impervious solid electrolyte. The rate of CH_4 oxidation was found to depend exponentially on catalyst potential and work function $e\Phi$ over wide (up to 0.8 eV) $e\Phi$ ranges. Within the same $e\Phi$ ranges the catalytic activation energy E varies linearly with $e\Phi$ and can be lowered from 40 kcal/mol to 11 kcal/mol. The observed behaviour can be accounted for within the framework of previous NEMCA studies, although in the present case, due to high operating temperatures, the role of direct electrocatalytic reactions is more pronounced.

INTRODUCTION

The effect of non-Faradaic electrochemical modification of catalytic activity (NEMCA) has been recently described for a number of catalytic reactions on transition metals deposited on Y_2O_3-doped ZrO_2 (*1–21*) and β''-Al_2O_3 solid electrolytes (*1, 2, 10, 11*). These studies have shown that when a current or potential is applied to solid electrolyte cells of the type

gaseous reactants, catalyst | solid electrolyte | counter electrode, O_2, (1)

the catalytic activity and selectivity of the catalyst film can be altered dramatically. The observed steady-state increase in catalytic rate can be up to a factor of 3×10^5 higher than the rate of supply of O^{2-} to the catalyst (*1, 2, 5*). Previous studies have shown that the increase in catalytic reaction rate can be up to a factor of 55 higher than the regular, open-circuit, catalytic rate. The main common findings of all previous NEMCA studies can be summarized as follows:

I. Over wide range of conditions catalytic rates depend exponentially on the Ohmic-drop-free (*1–19*) catalyst potential V_{WR} with respect to a reference electrode,

$$\ln(r/r_0) = \alpha F(V_{WR} - V^*_{WR})/RT, \quad (2)$$

where r_0 is the regular, i.e., open-circuit, catalytic rate and α and V^*_{WR} are catalyst- and reaction-specific constants. The parameter α typically takes values between -1 and 1. Depending on their sign, catalytic reactions can be termed electrophobic ($\alpha > 0$) or electrophilic ($\alpha < 0$) (*1, 2*).

As shown recently, both theoretically (*2, 5, 6*) and experimentally by means of a Kelvin probe (*1, 11*) the emf of solid electrolyte cells with metal electrodes provides a direct measure of the difference in work function of the catalyst and reference electrode gas-exposed surfaces. Thus, when the catalyst potential V_{WR} is changed by ΔV_{WR}, either by changing the composition of the gas in contact with the catalyst or by polarizing the catalyst–solid electrolyte interface, then the average catalyst surface work function $e\Phi$ changes by

0021-9517/93 $5.00

$$\Delta e\Phi = e\Delta V_{WR}. \quad (3)$$

Consequently Eq. (2) can also be written as

$$\ln(r/r_0) = \alpha e(\Phi - \Phi^*)/k_b T, \quad (4)$$

where Φ^* is again a catalyst- and reaction-specific constant.

II. The order of magnitude (typically $1-10^5$) of the absolute value $|\Lambda|$ of the enhancement Factor Λ defined as:

$$\Lambda = \Delta r/(I/2F), \quad (5)$$

where Δr is the change in catalytic reaction rate and $I/2F$ is the rate of supply ($I > 0$) or removal ($I < 0$) of O^{2-} to or from the catalyst, can be estimated from

$$|\Lambda| = 2Fr_0/I_0, \quad (6)$$

where I_0 is the exchange current of the catalyst–solid electrolyte interface. Thus, in order to observe a strong non-Faradaic enhancement, i.e., $|\Lambda| \gg 1$, highly polarizable, i.e., low I_0 catalyst–solid electrolyte interfaces are required. This observation is of particular importance for the present work, since the high operating temperatures required to obtain a measurable open-circuit catalytic rate r_0 value also caused high (typically 5–20 mA) I_0 values, and, therefore, $|\Lambda|$ was limited to low (typically less than 5) values.

III. The catalytic rate relaxation time constants during galvanostatic transients are typically of the order of $2FN/I$ where N, expressed in g-atom, is the total gas-exposed catalyst film surface area. This shows that NEMCA changes the catalytic properties of the entire catalyst surface and is not restricted to the vicinity of the three-phase boundaries (tpb) solid electrolyte–catalyst–gas.

The above observations have been interpreted semiquantitatively on the basis of the changes induced in the strength of chemisorptive bonds of reactant and intermediates due to an electrochemically induced and controlled ion spillover and due to the concomitant change in catalyst work function. That ion spillover is indeed taking place under NEMCA conditions is strongly supported both by previous *in situ* XPS measurements of Arakawa *et al.* (*22, 23*) on Ag deposited on yttria-stabilized zirconia (YSZ) and also by the excellent agreement of the computed dipole moment of Na spillover atoms on Pt under NEMCA conditions using β''-Al_2O_3 (*2, 11*) with literature values for Na/Pt(111) (*2, 24*). That the strength of chemisorptive bonds is significantly affected under NEMCA conditions has been shown recently by studying the kinetics of oxygen adsorption and desorption on Ag/YSZ (*18*).

The oxidation of methane in solid electrolyte cells has been the focal point of numerous recent studies aiming at obtaining high selectivity to oxidative coupling products, i.e., ethane and ethylene. Work in this area has been reviewed very recently (*25*).

It was also found very recently that the YSZ solid electrolyte is by itself a reasonably active and selective catalyst at temperatures above 700°C (*26, 27*).

The present work is part of an investigation attempting to utilize NEMCA to promote methane conversion to C_2 hydrocarbons on metal and metal oxide catalysts (*2, 28*). Due to the high catalytic activity of Pt relative to YSZ and due to the high ratio of surface areas of Pt and YSZ used in the present investigation, the only detectable products were CO_2 and H_2O. Thus the catalytic influence of YSZ is negligible under the conditions of the present investigation.

Several workers have studied the oxidation of CH_4 on Pt (*29–35*) and have shown it to be a structure-sensitive reaction (*33, 34*). Although some authors have fitted their data at lower temperatures using Langmuir–Hinshelwood-type rate expressions involving adsorbed oxygen and methane (*31*), it is generally believed today that methane adsorption is weak and can occur to a significant extent only after chemisorbed oxygen has abstracted one hydrogen atom to form CH_3 and other C_1 fragments on the surface. The bonding of C_1 fragments on Pt

and other transition metal surfaces has been the object of some outstanding recent studies involving molecular orbital calculations (*36, 37*).

In a recent study Eng and Stoukides have explored the effect of electrochemical O^{2-} pumping to Pt surfaces ($I > 0$) during CH_4 oxidation (*20*). Enhancement factor Λ values up to 5 were measured during this interesting exploratory study which utilized a two-electrode system. In the present study a three-electrode system is utilized to measure catalyst potential and work function changes (*2*) and the effect of both positive and negative currents on the rate and activation energy is studied in detail.

EXPERIMENTAL

The apparatus utilizing on line gas chromatography, mass spectrometry (Balzers QMG-311) and IR-spectroscopy (Anarad 500 analyzers for CH_4 and CO_2) has been described in previous papers (*2–10*). The YSZ (8 mol% Y_2O_3 in ZrO_2) atmospheric pressure, continuous flow well-mixed (CSTR) reactor has a volume of 30 cm^3 and has also been described previously (*2–6*). Results reported here were typically obtained with total flowrates of 1–3 cm^3 STP/s. Reactants were Air Liquide certified standard CH_4 in N_2 and Air Liquide 20 mol% O_2 in N_2. They could be further diluted in pure N_2 (99.99%).

The porous Pt catalyst film was deposited on the inside bottom wall of the stabilized zirconia tube as described previously (*2–4*), i.e., by applying a thin coating of Engelhard A1121 Pt paste followed by drying and calcining in air first for 2 h at 450°C and then for 30 min at 850°C. The thickness of the Pt film was of the order of 5 μm. The superficial surface area was 2 cm^2 and the true surface area was of the order of 50 cm^2 as measured by a surface titration technique utilizing O_2 and C_2H_4 described previously (*2–5*). Two Pt catalyst films termed C1 and C2 were used in the course of this investigation and both gave similar results. Table 1 lists their active catalytic surface areas and also the exchange current I_0 of the catalyst–solid electrolyte interface. The experimental procedure for extracting I_0 from current vs overpotential (Tafel) plots has been described in detail previously (*2, 5, 6*).

TABLE 1

Catalyst Surface Area and Apparent Exchange Current and Transfer Coefficients

Anodic operation ($I > 0$)			Cathodic operation ($I < 0$)	
T (°C)	I_0 (mA)	α_a	I_0/(mA)	α_c
	Catalyst C1			
	$N = 9 \times 10^{-8}$ g-atom Pt			
685	2.0	0.95	0.38	0.5
715	5.5	0.7	0.6	0.55
730	8.0	1.0	0.8	0.65
740	11.5	0.8	1.0	0.65
	Catalyst C2			
	$N = 6 \times 10^{-8}$ g-atom Pt			
650	0.8	0.75	0.2	0.55
675	1.6	0.8	0.3	0.45
700	1.8	0.65	0.5	0.4
735	3.5	0.6	1.5	0.4

Two similar Pt films were deposited on the outside wall of the stabilized zirconia tube which was exposed to ambient air (Fig. 1) and served as counter and reference electrodes, respectively. In the course of the experiments both galvanostatic and potentiostatic operation was used and both gave

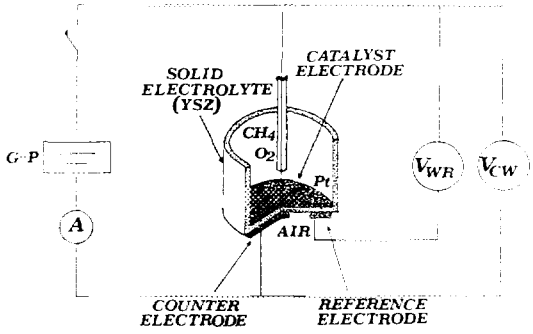

FIG. 1. Schematic cross-section of the bottom of the closed-flat YSZ tube showing the catalyst, counter, and reference electrode configuration; G–P: galvanostat-potentiostat.

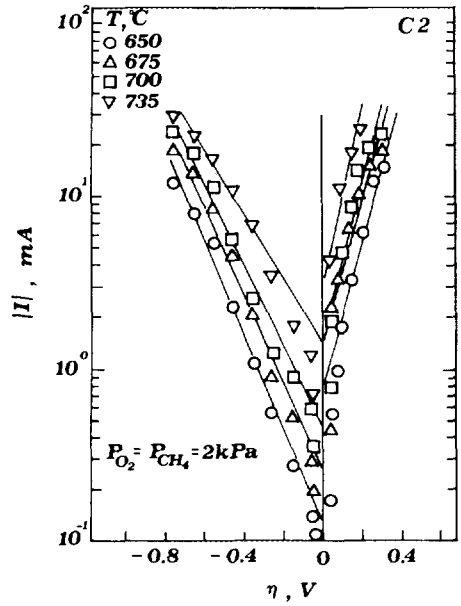

FIG. 2. Effect of catalyst overpotential η on current I (Tafel plots), catalyst C2.

similar results. In the galvanostatic mode a constant current I is applied between the catalyst and counter electrodes while monitoring the Ohmic-drop-free (*2, 5, 6*) potential V_{WR} between the catalyst and the reference air/Pt electrode. In the potentiostatic mode a constant potential V_{WR} is applied between the catalyst and the reference electrode while monitoring the current I between the catalyst and the counter electrode.

RESULTS

Exchange current measurements. Figure 2 shows the observed dependence of current I on catalyst overpotential η for constant gaseous composition ($P_{CH_4} = P_{O_2} = 2$ kPa). The overpotential η is defined from

$$\eta = V_{WR} - V^0_{WR}, \qquad (7)$$

where V^0_{WR} is the open-circuit ($I = 0$) value of V_{WR}, i.e., the open-circuit emf. The exchange current I_0 is obtained by extrapolating the linear ln I vs η (Tafel) part of the curves to $\eta = 0$ (*2, 5, 6*). As shown in Fig. 2 this extrapolation for $I > 0$, i.e., O^{2-} supply to the catalyst, leads to larger apparent I_0 values than those obtained by extrapolation for $I < 0$ (Table 1). This is different from the symmetric behaviour observed in absence of CH_4 (*2*) and is due to the substantially different values of the anodic and cathodic transfer coefficients α_a and α_c, respectively (Table 1). The latter suggests the possibility of different anodic and cathodic electrocatalytic reactions, which is also corroborated by the kinetic results, as analyzed in the Discussion. Nevertheless, the temperature dependence of I_0 extracted either from $I > 0$ or from $I < 0$ suggests in both cases an apparent activation energy of 40 kcal/mole, i.e., almost identical to the value measured in absence of CH_4 (*2, 5*) where the dominant electrocatalytic reaction taking place at the three-phase boundaries (tpb) is (*2*)

$$O^{2-} \leftrightharpoons O(a) + 2e^-, \qquad (8)$$

where O(a) denotes oxygen adsorbed on the Pt surface near the tpb YSZ-Pt-gas.

As shown in Table 1 the anodic transfer coefficient α_a (*2*) is consistently higher than the cathodic transfer coefficient α_c. As analyzed in the Discussion, the observed behaviour can be rationalized by considering, in addition to reaction (8), the occurrence of two other electrocatalytic, i.e., charge transfer, reactions involving the direct participation of CH_4.

From the viewpoint of NEMCA, however, the exact determination of the charge transfer steps is not crucial, as the only parameter of practical importance is the exchange current I_0 which determines via Eq. (6), i.e.,

$$|\Lambda| \approx 2Fr_0/I_0, \qquad (6)$$

the expected magnitude of the absolute value of the enhancement factor Λ (*2*). Due to the high operating temperatures of the present study (600–750°C), which were dictated by the low reactivity of CH_4 and the low (~50 cm^2) Pt-catalyst surface area, the measured I_0 values were high, i.e., on the order 1 mA. This, in conjunction with Eq. (6), implies that low $|\Lambda|$ values are to be

expected, in agreement with the exploratory study of Eng and Stoukides and with the present kinetic results as shown below.

Open-circuit and closed-circuit kinetics. Figures 3a and 3b show the effect of P_{CH_4} and P_{O_2} on the regular, i.e., open-circuit catalytic rate. The rate is clearly first-order in CH_4 and practically zeroth-order in oxygen for $P_{O_2} > 4$ kPa. This behaviour is consistent with an Eley–Rideal-type mechanism involving gaseous CH_4 and atomically adsorbed oxygen.

Figures 3c and 3d also show the effect of P_{CH_4} and P_{O_2} on the rate r under closed-circuit, i.e., NEMCA conditions, both for a positive and for a negative value of η. In both cases the rate increases substantially but, interestingly, the kinetic effect of the reactants remains qualitatively the same. Figures 3a through 3d were obtained with the catalyst film labeled C1, but the behaviour was practically the same with the catalyst film C2.

Galvanostatic transients. Figure 4 shows typical galvanostatic transients for anodic ($I > 0$) operation, i.e., it depicts the transient effect on the rate of step changes in applied current. The circuit is initially open ($I = 0$) and the corresponding steady-state catalytic rate r_0 for the reaction

$$CH_4 + 2O_2 \rightarrow CO_2 + 2H_2O \qquad (9)$$

is 1.2×10^{-8} g-atom O/s (To keep the notation consistent with previous NEMCA studies we express rates in terms of g-atom O/s or, when O_2 is not involved as a reactant or product, in terms of g-equivalent O/s). The catalyst potential V_{WR} has initially the value of -800 mV.

At $t = 0$ the galvanostat is used to apply a constant current $I = 3$ mA, so that O^{2-} ions are supplied to the catalyst at a steady-state rate $I/2F = 1.56 \times 10^{-8}$ g-atom O/s. This causes a 167% increase in r ($\rho = r/r_0 = 2.67$). The increase $\Delta r = 2 \times 10^{-8}$ g-atom O/s is 28% higher than $I/2F$, thus $\Lambda = 1.28$.

Subsequently (Fig. 4) the circuit is opened ($I = 0$) and the rate r is restored to its initial value r_0, indicating the reversibility of the process.

The procedure is then repeated with $I = 5$ mA. This causes a 308% increase in the rate ($\rho = 4.08$). The rate increase $\Delta r = 3.7 \times 10^{-8}$ g-atom O/s is 42% higher than the rate $I/2F$ of O^{2-} supply to the catalyst ($\Lambda \approx 1.42$).

Finally the procedure is repeated with $I = 10$ mA which causes a 660% increase in the rate ($\rho = 7.6$) and a Λ value of 1.54.

Figure 5 shows typical galvanostatic transients for cathodic ($I < 0$) operation. For $t < 0$ the circuit is open ($I = 0$) and the open-circuit catalytic rate r_0 is 0.6×10^{-8} g-atom O/s. At $t = 0$ the galvanostat is used to apply a current $I = -5.5$ mA, thus O^{2-} is *removed* from the catalyst at a steady-state rate of 2.85×10^{-8} g-atom O/s. Surprisingly, this causes a 260% *increase* in the rate of CO_2 production ($\rho = 3.6$). The rate increase $\Delta r = 1.6 \times 10^{-8}$ g-atom O/s equals 56% of the rate of O^{2-} removal ($\Lambda = -0.56$). Upon current interruption the rate relaxes back to its initial value.

The procedure is then repeated three times (Fig. 5) with $I = -8.8$, -12.7, and -16 mA, respectively. The corresponding rate *increases* are 3.2×10^{-8}, 5.3×10^{-8}, and 6.2×10^{-8} g-atom O/s. The corresponding ρ ($=r/r_0$) values are 6.3, 9.8, and 11.3, respectively, while the corresponding Λ values are -0.70, -0.81, and -0.75, respectively.

As shown on Figs. 4 and 5, the relaxation time constants τ (defined as the time required for the rate increase Δr to reach 63% of its final steady-state value) are between 7 and 20 s and decrease with increasing I, in qualitative agreement with $\tau \sim 2FN/I$ (2), where N is the independently measured catalyst surface area expressed in metal g-atom (Table 1). This observation provides strong evidence that, despite the small measured values of Λ, the rate increases are due to a rate enhancement over the entire catalyst surface (NEMCA) and not due to a rate enhancement at the tpb only, in which case τ would be negligible since the rate would

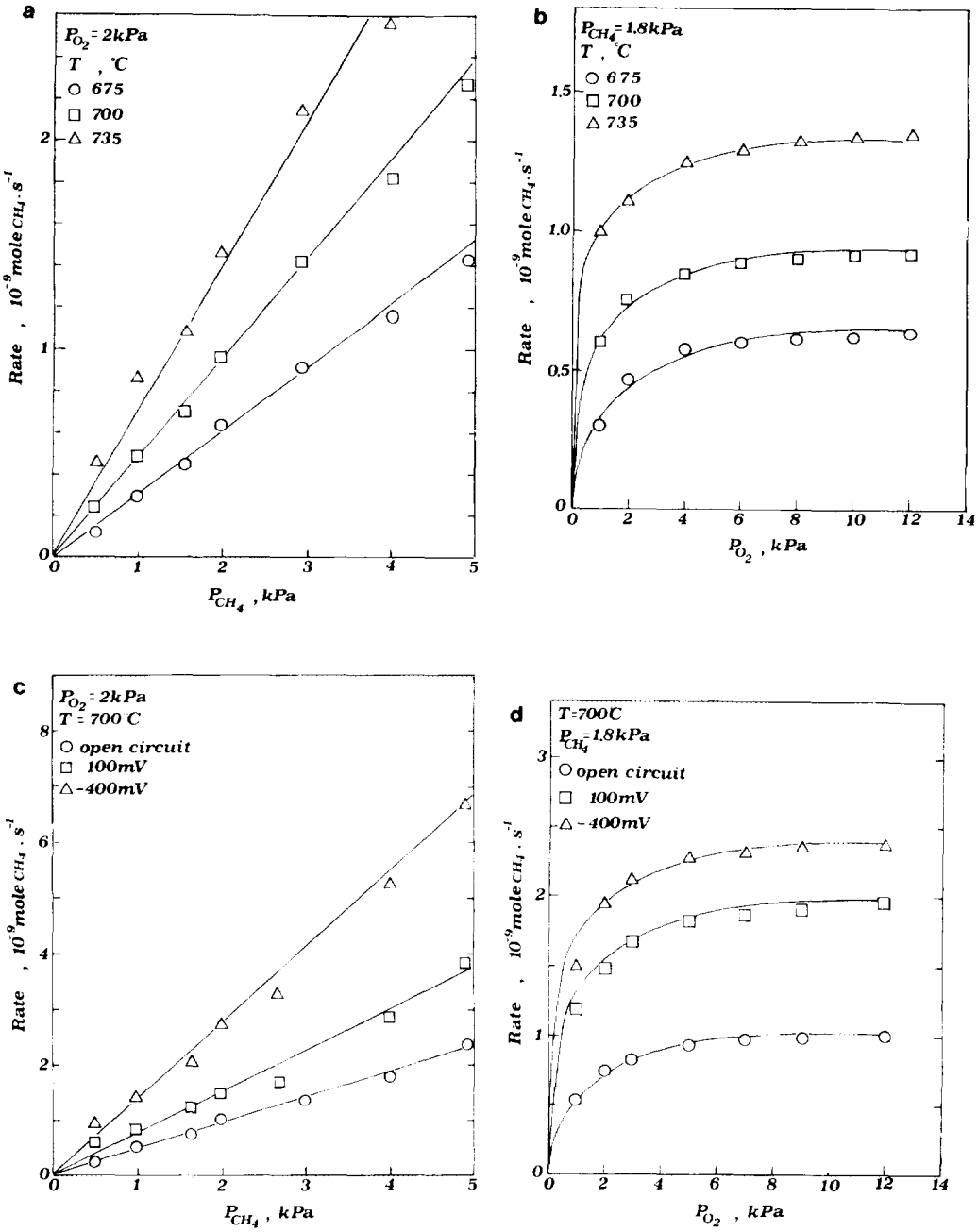

FIG. 3. (a) Effect of P_{CH_4} on the open-circuit rate of oxidation. (b) Effect of P_{O_2} on the open-circuit rate of oxidation. (c) Effect of P_{CH_4} on the rate of oxidation for $\eta = 0$, 100 mV and -400 mV. (d) Effect of P_{O_2} on the rate of oxidation for $\eta = 0$, 100 mV and -400 mV.

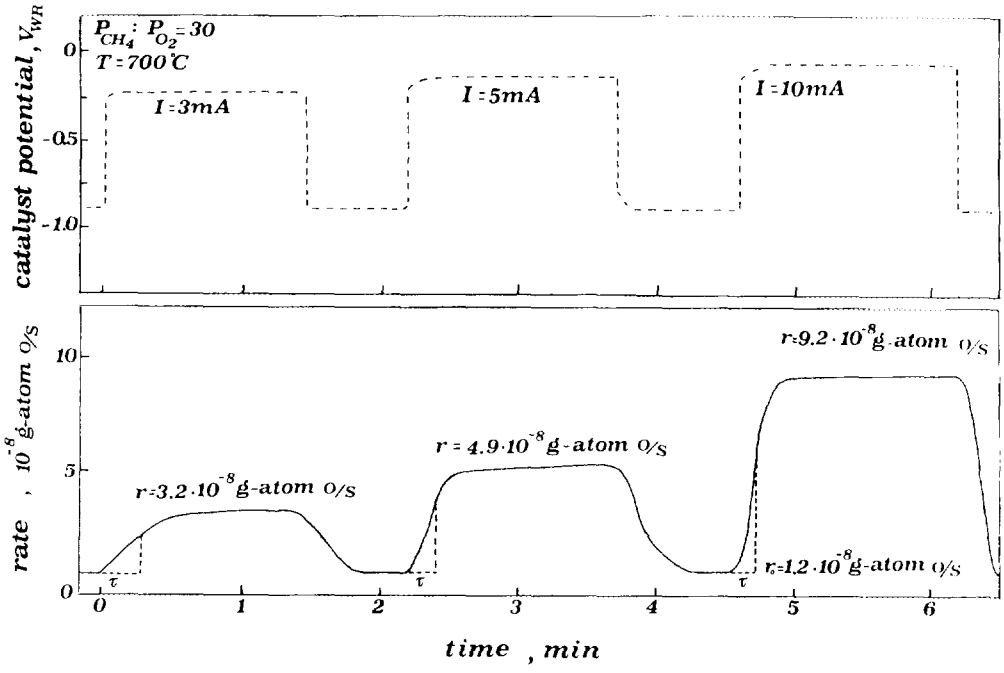

FIG. 4. Effect of step changes in applied positive current on catalyst potential V_{WR} and on the rate of CO_2 production; P_{O_2} = 0.2 kPa, P_{CH_4} = 6 kPa, volumetric flowrate F_v = 1 cm^3 STP/s, catalyst Cl; see text for discussion.

follow the step changes of the applied current (electrocatalysis).

One point requiring attention is that due to the high values of current used in the present study, τ is much shorter than in previous NEMCA studies (*1–19*) where the applied currents were of the order of 5–50 μA and τ was of the order of several min. Thus in the present work care must be taken so that the measured rate transients are not influenced significantly by the reactor residence time distribution. On the assumption of an ideal CSTR one computes that the mean residence time τ_R is 8.4, 4.2, and 2.1 s, respectively, for a volumetric flowrate F_v of 1, 2, and 3 cm^3 STP/s, i.e., τ_R is close to the measured τ values. To investigate this in detail a series of galvanostatic transients were obtained under identical conditions but with varying F_v between 1 and 4 cm^3 STP/s (Fig. 6). It was found that τ is not significantly influenced by F_v and τ_R and, therefore, the transients shown on Figs. 4, 5, and 6 reflect the transient behaviour of the catalyst and not of the reactor. This can also be verified by examining Fig. 6, which shows that, upon current interruption, r returns to its open-circuit value r_0 within 2–5 s, i.e., much faster than it increases from r_0 to r upon current imposition, i.e., faster than τ.

Steady-state effect of current. Figure 7 shows the steady-state effect of current I on the increase in the rate of CO_2 production. Straight lines passing through the (0, 0) point on this diagram are, by definition, constant enhancement factor Λ lines. As shown in the figure, Λ values up to 3 have been measured for $I > 0$, in qualitative agreement with Eng and Stoukides (*20*), who measured Λ values up to 5. However, quite often and in particular for low $CH_4 : O_2$ ratios, Λ was found to be less than unity for $I > 0$ (Fig. 7). For $I < 0$

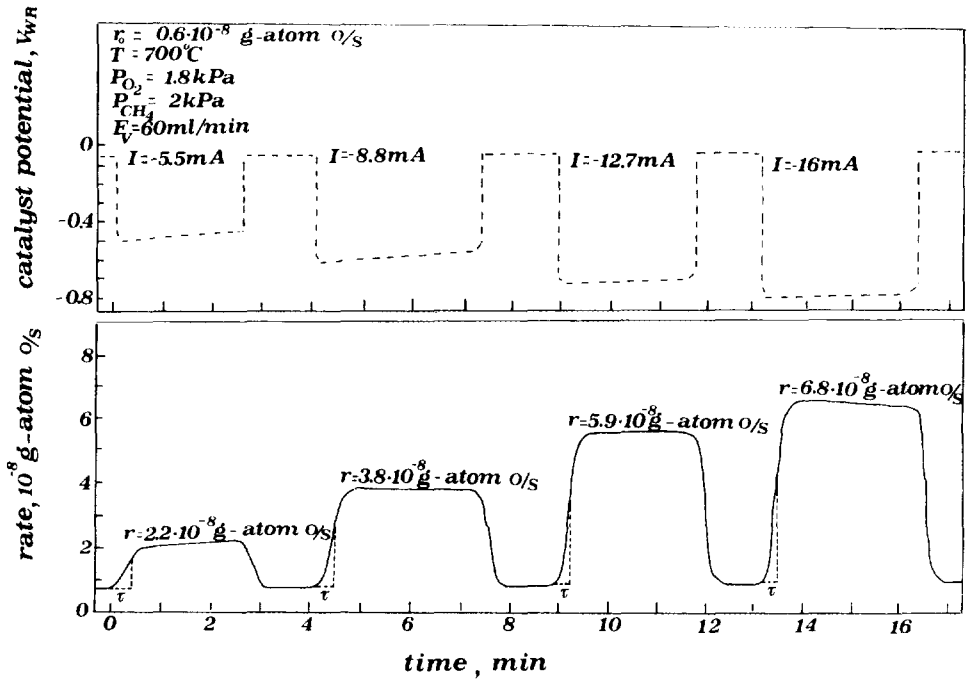

FIG. 5. Effect of step changes in applied negative current on catalyst potential V_{WR} and on the rate of CO_2 production, catalyst C1; see text for discussion.

the enhancement factor Λ is usually of the order of -1 (Fig. 7).

These low $|\Lambda|$ values fit nicely with the approximate expression

$$|\Lambda| \approx 2Fr_0/I_0, \qquad (6)$$

which has been derived analytically (*2, 5, 6*) and shown to describe very well the measured Λ values of all previous NEMCA studies (*1–19*) as shown in Figs. 8a and 8b. Despite this very good agreement it is very likely, as shown in the Discussion, that direct electrocatalysis in addition to NEMCA, is responsible for the observed behavior.

Effect of catalyst potential and workfunction. Figure 9 shows the effect of catalyst potential V_{WR} and, equivalently (*1, 2, 11*), work function change $\Delta e\Phi$ on the rate of CO_2 production for a low (1 : 1) CH_4 to O_2 ratio and for both catalyst films studied.

Increasing V_{WR} above its open-circuit value (i.e., $I > 0$, $\eta > 0$, $\Delta e\Phi > 0$) causes an exponential increase in reaction rate, which can be approximated by

$$\ln(r/r_0) = \alpha e(\Phi - \Phi^*)/k_bT, \qquad (10)$$

with $\alpha \approx 0.7$. Therefore, for $V_{WR} > V^0_{WR}$ the reaction exhibits electrophobic behaviour (*1, 2, 5, 6*), i.e., $\alpha > 0$ with ρ values up to 7. This behaviour is much more pronounced for high (40 : 1 and 20 : 1) CH_4 to O_2 ratios (Fig. 10). The slope α is now near 0.4 and ρ values up to 70 are obtained.

Decreasing V_{WR} below V^0_{WR} (i.e., $I < 0$, $\eta < 0$, $\Delta e\Phi < 0$) causes again an exponential increase in catalytic rate conforming again to Eq. (9) with $\alpha \approx -0.35$ (Fig. 9). Thus for $V_{WR} < V^0_{WR}$ the reaction exhibits electrophilic behaviour with ρ values up to 60. The rate enhancement ratio ρ values shown on Figs. 9 and 10 are the highest ρ values measured so far in NEMCA studies.

Effect of catalyst potential and work function on activation energy and preexponen-

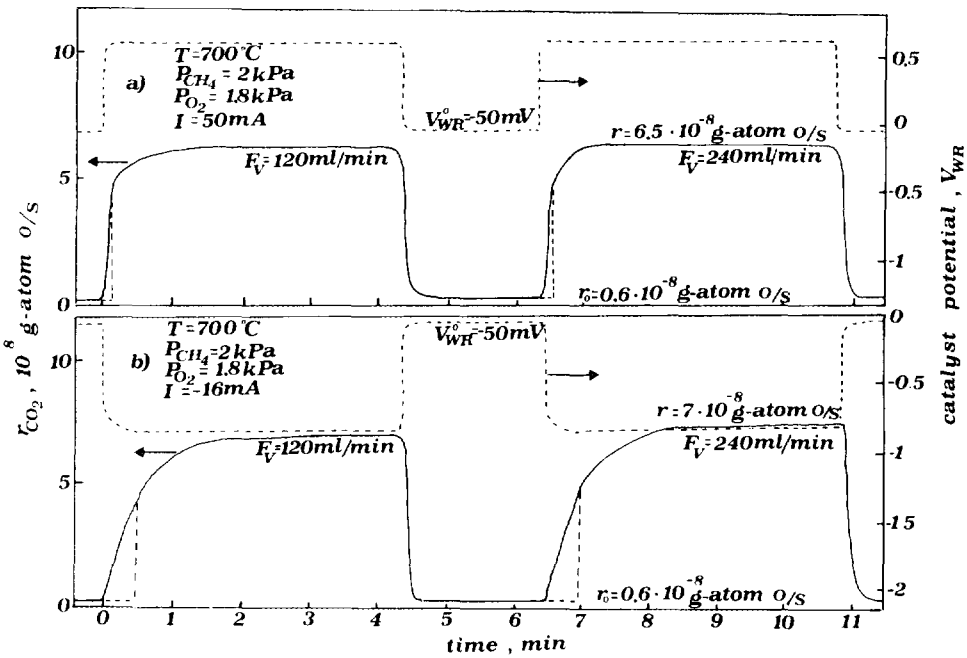

FIG. 6. Effect of step changes in applied positive and negative currents on V_{WR} and r at two different volumetric flowrate F_v showing that τ is influenced by I but not by F_v.

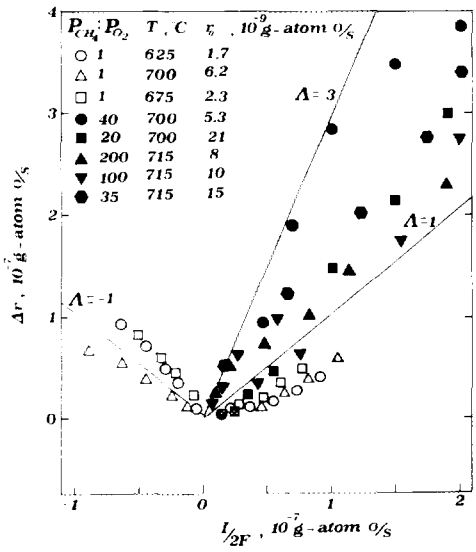

FIG. 7. Steady-state effect of applied current on the increase in the rate of oxygen consumption.

tial factor. By studying the temperature dependence of r in the range 625 to 750°C at various fixed values of V_{WR} or $\Delta e\Phi$ and by using standard Arrhenius ln r vs $1/T$ plots (Fig. 11), one can study the effect of V_{WR} and $\Delta e\Phi$ on the activation energy E and preexponential factor K^0 of H_2O kinetic constant K, where

$$r = KP_{CH_4}; \qquad K = K^0 \exp(-E/k_bT). \quad (4)$$

The study was performed for low CH_4-to-O_2 ratios (1 : 1) to ensure that the rate expression (11) remains valid. The results of this study are presented in Fig. 12. Interestingly, open-circuit operation corresponds to the maximum activation energy (1.74 eV/molecule or 40 kcal/mole) and, also, maximum preexponential factor.

There is a linear decrease in E with increasing, but also with decreasing, V_{WR} and $e\Phi$,

$$E = E^0 + \alpha_H \Delta e\Phi, \quad (12)$$

where $\alpha_H = -4.5$ for $\Delta e\Phi > 0$, i.e., $V_{WR} > V^0_{WR}$ and $\alpha_H = +1$ for $\Delta e\Phi < 0$, i.e., $V_{WR} < V^0_{WR}$. As shown in Fig. 12, E decreases from 40 kcal/mole down to 11 kcal/mole upon increasing $e\Phi$ and down to 23 kcal/mole upon decreasing $e\Phi$.

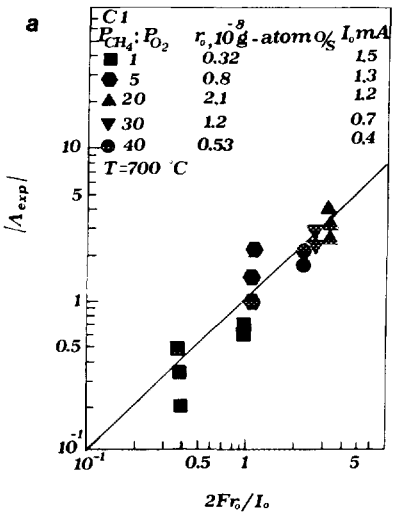

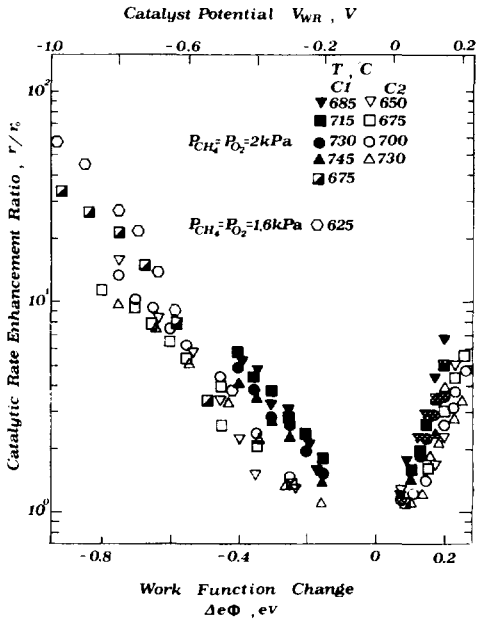

FIG. 9. Effect of catalyst potential V_{WR} and work function change (vs $I = 0$) on the rate of CH_4 oxidation for a low (1 : 1) CH_4 to O_2 feed ratio. Maximum CH_4 conversion is 4%; F_v = 1 cm³ STP/s.

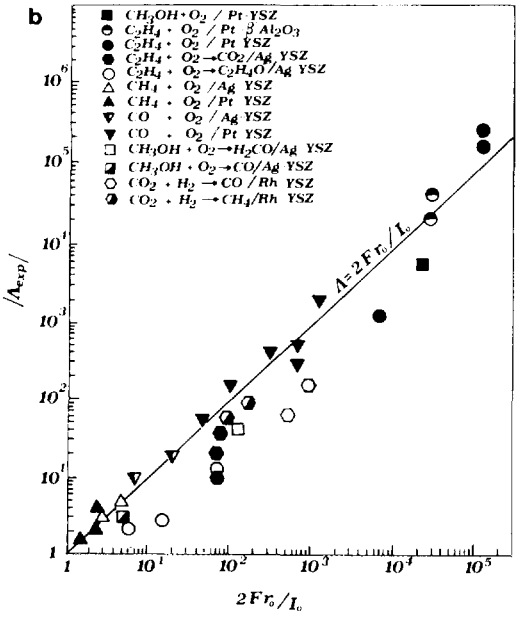

FIG. 8. Effect of the parameter $2Fr_0/I_0$ on the absolute value $|\Lambda|$ of the enhancement factor Λ: (a) present study and (b) present and previous NEMCA studies (*1–19*).

As also shown on Fig. 12, there is a partly compensating change in the preexponential factor K^0, the logarithm of which also varies linearly with $e\Phi$ according to

$$\ln(K^0/K^0_0) = \alpha_s \Delta e\Phi/k_b T, \qquad (13)$$

where K^0_0 is the open-circuit K^0 value and α_s equals -3.9 for $V_{WR} > V^0_{WR}$ and 0.7 for $V_{WR} < V^0_{WR}$. The above α_s and α_H values satisfy reasonably well the equation

$$\alpha = \alpha_s - \alpha_H, \qquad (14)$$

where α is the NEMCA coefficient (Eq. 10). This confirms the consistency of the extracted activation energy and preexponential factor values.

Linear variations in catalytic activation energy E and ln K^0 with changing catalyst work function $e\Phi$ have also been observed in previous NEMCA studies (*2, 5, 6*) and attributed to linear variations in heats of adsorption with changing $e\Phi$ (*1, 2, 5, 38*). It is

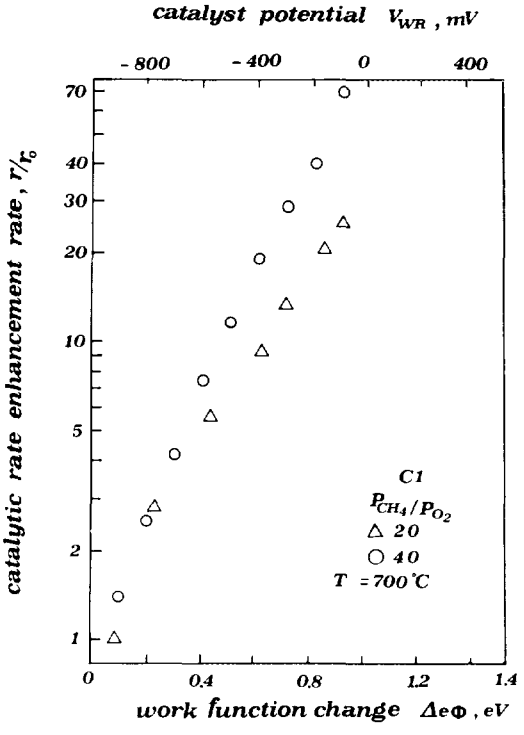

FIG. 10. Effect of catalyst potential and work function change (vs $I = 0$) for high (20 : 1) and (40 : 1) CH_4 to O_2 feed ratios; maximum O_2 conversion is 62%; F_v = 1 cm³ STP/s; feed conditions: (○), P_{CH_4} = 10 kPa, P_{O_2} = 0.25 kPa; (Δ), P_{CH_4} = 10 kPa, P_{O_2} = 0.5 kPa.

worth noting that Firth and Holland, who studied CH_4 oxidation on Pt, Rd, Rh, and Ir, also reported a linear decrease in the reaction activation energy with decreasing metal–oxygen bond energy with a slope of 1 (*29*).

DISCUSSION

The present study shows that the activity of Pt for CH_4 oxidation can be enhanced by up to a factor of 70 by interfacing Pt with yttria-stabilized zirconia (YSZ) and electrochemically supplying or removing oxide ions O^{2-} to or from the catalyst surface. For $I > 0$, i.e., $V_{WR} > V^0_{WR}$, the rate of CO_2 formation increases exponentially with increasing catalyst potential and work function with a concomitant linear decrease in activation energy from 40 to 11 kcal/mole. For $I < 0$, $V_{WR} < V^0_{WR}$ the rate of CO_2 formation increases exponentially with decreasing V_{WR} and $e\Phi$ with a concomitant linear decrease in activation energy from 40 to 23 kcal/mole. The observed rate enhancement ratio ($\rho = r/r_0$) values of 70 are the highest observed so far in NEMCA studies (*1–21*). The highest previously reported ρ value was 55 for the case of C_2H_4 oxidation on Pt (*1, 2, 5*). However, due to the much higher operating temperature of the present study (600 to 750°C) which was dictated by the low reactivity of Pt for the oxidation of CH_4, the rates of *electrocatalytic* reactions are comparable with the catalytic rate of CH_4 oxidation. Consequently, as analyzed below, electrocatalysis, in addition to NEMCA, affects significantly the observed kinetic behaviour.

Kinetics and literature. The observed open-circuit kinetic behaviour is in good agreement with previous studies both regarding the first-order rate dependence on P_{CH_4} (Fig. 3a) and also the near zeroth-order rate dependence on P_{O_2} (Fig. 3b). For $P_{O_2} <$ 4 kPa there is a shift to positive-order kinetics in O_2, as should be expected due to the higher operating temperatures and to the concomitant decrease in oxygen coverage for low P_{O_2}, also in agreement with literature (*31*). Also, the open-circuit activation energy value E^0 = 1.74 eV/atom = 40 kcal/mole is in good agreement with previous studies (*29–34*). Most of the reported activation energy values fall between 26 and 40 kcal/mole. Recent studies (*33, 34*) have provided strong evidence that CH_4 oxidation on Pt supported on γ-Al_2O_3 is a structure-sensitive reaction. Activation energy values of the order 25–28 kcal/mole have been attributed to reaction on "particulate" Pt, while E values of 34–38 kcal/mole are attributed to a "dispersed" phase (*30, 33, 34*). On the basis of this activation energy assignment and in view of the fact that, as shown by SEM (*2*), the Pt film used in the present study consists of crystallites 1–2 μm in diameter, one would expect an E value closer to that attributed to reaction on "particu-

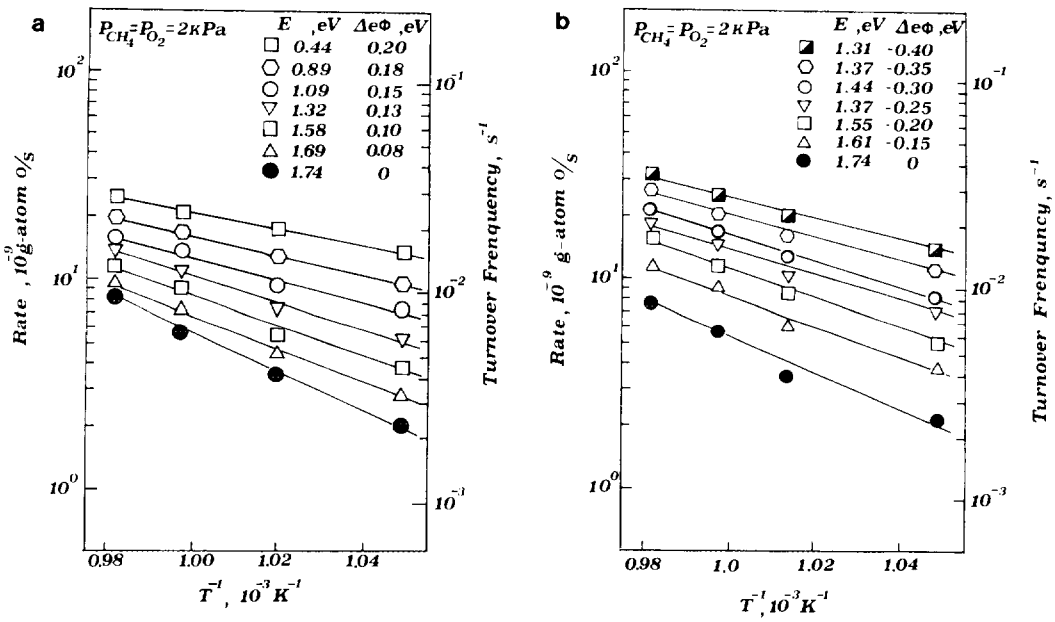

FIG. 11. Arrhenius plots at fixed $\Delta e\Phi$ ($=e\Delta V_{WR}$) values (vs $I = 0$) for anodic ($I > 0$, $\Delta e\Phi > 0$) (a) and cathodic ($I < 0$, $\Delta e\Phi < 0$) operation (b).

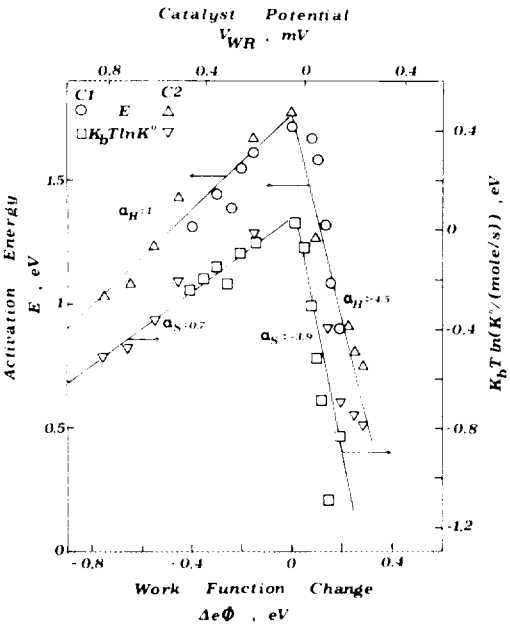

FIG. 12. Effect of catalyst potential V_{WR} and work function change (vs $I = 0$) on the activation energy E and preexponential factor K^0 of the kinetic constant K of CH_4 oxidation to CO_2; an average T value of 948 K is used in the RHS ordinate.

late" Pt. This however, was not the case and this point deserves further investigation. Comparison of turnover frequencies (TOF) is not straightforward, since previous studies very typically limited to temperatures below 500°C and also since there is very considerable scattering in previously reported TOF values (*33, 34*). Extrapolation of the kinetics and activation energies reported in these previous studies to the conditions of the present investigation lead to TOF values one to two orders of magnitude higher than the measured ones, but this again may be a result of the structure sensitivity of the CH_4 oxidation reaction (*33, 34*).

Role of YSZ and of homogeneous reactions. The good qualitative agreement between this and previous studies regarding the effect of P_{CH_4}, P_{O_2}, and T on the oxidation rate seems to indicate that the presence of the YSZ surface, on which the Pt film is supported, plays no important role in the observed kinetics and thus the catalytic reaction takes place on the gas-exposed Pt surface only. It is worth noting that recent studies (*26, 27*) have shown that YSZ is itself

a decent catalyst for the partial oxidation of CH_4 to C_2 hydrocarbons and CO_2 at temperatures above 700°C. Also Eng and Stoukides, who performed a limited study of CH_4 oxidation on Pt films deposited on YSZ at temperatures above 650°C, found the presence of trace C_2 hydrocarbons in the products (*27*). The extent to which C_2 hydrocarbons can be found in the products clearly depends on the ratio of YSZ and Pt surfaces present in the reactor and also on temperature. The fact that no measurable amounts of CO or C_2 hydrocarbons were detected in the present study, together with the good qualitative agreement of the kinetics with previous studies of CH_4 oxidation on Pt, shows that YSZ and homogeneous gas-phase reactions played a very limited, if any, role in the observed kinetic behaviour.

Electrocatalysis and the role of the exchange current I_0. Before attempting to rationalize the dramatic changes induced in catalytic activity and activation energy during electrochemical O^{2-} pumping on the basis of mechanistic considerations it is important to first point out the consequences of the substantially higher operating temperature range used in this study (660–750°C) in comparison to previous NEMCA studies (200–500°C).

The first, and almost unavoidable, consequence of the high operating temperature is the high values (typically 1 mA) of the exchange current I_0 (Fig. 2). This parameter increases exponentially with temperature with an apparent activation energy of 40 kcal/mol for Pt/YSZ and 20 kcal/mol for Ag/YSZ (*2*). The present value of 40 kcal/mol measured in presence of reacting $CH_4 - O_2$ mixtures is in very good agreement with literature values measured in presence of O_2 only (*2*).

Previous NEMCA studies have shown that one can estimate the order of magnitude of the absolute value $|\Lambda|$ of the enhancement factor Λ from

$$|\Lambda| \approx 2Fr_0/I_0. \tag{6}$$

The derivation of this approximate expression has been presented previously (*2, 5, 6*). It is obtained by combining the Butler–Volmer equation

$$\ln(I/I_0) = \alpha_a F(V_{WR} - V^0_{WR})/RT - \alpha_c F(V_{WR} - V^0_{WR})/RT \tag{15}$$

(where α_a, α_c are the anodic and cathodic transfer coefficients, respectively) with the exponential catalytic rate–V_{WR} (or $e\Phi$) relationship established in this and in previous NEMCA studies (*1–19*), i.e.,

$$\ln(r/r_0) = \alpha F(V_{WR} - V^*_{WR})/RT, \tag{16}$$

and by setting $\alpha \approx \alpha_a$ or α_c and $V^*_{WR} \approx V^0_{WR}$. These are, of course, only approximations, which cause the scattering shown on Fig. 8b where measured Λ values for 13 catalytic reactions are compared with Eq. (6). As shown in the figure there is very good agreement over more than five orders of magnitude and the oxidation of CH_4 on Pt also falls on this line. However, due to the high operating T and high I_0 values, the measured Λ values are small (Eq. 6), typically less than 3.

The physical origin of this can be understood as follows: When I_0 is high (say 1 mA), then currents I of 20 mA are required to cause a substantial catalyst overpotential $\eta = V_{WR} - V^0_{WR}$ of, say, 400 mV (Fig. 2 or Eq. 15). However, the O^{2-} flux I/2F corresponding to 20 mA is 1.03×10^{-7} g-atom O/s, i.e., larger than the open-circuit catalytic rate r_0 which is typically 10^{-8}–10^{-9} g-atom O/s (Figs. 3–6). Thus even a fiftyfold rate increase will give Λ values of order 0.5 to 5, respectively.

An equivalent way to illustrate this is to rewrite Eq. (6) as

$$|\Lambda| = \frac{|\Delta r|}{|I/2F|} \approx \frac{r_0}{(I_0/2F)}. \tag{17}$$

The RHS of Eq. (17) is of the order of 0.2, unlike previous NEMCA studies where it was typically 10^2–10^5 (*1–19*). Therefore it is the combination of the slow kinetics of CH_4 oxidation (low r_0) and high operating tem-

peratures (high I_0) which dictate the low magnitude of $|\Lambda|$.

Since both r_0 and I_0 are strongly temperature dependent, it would appear that one could increase $r_0/(I_0/2F)$ by appropriate choice of temperature. This, however, cannot be done, since both r_0 and I_0 increase with practically the same activation energy of 39–40 kcal/mole, a fact which, as discussed below, is probably not coincidental.

It would appear that another possible strategy to increase $r_0/(I_0/2F)$ would be to increase the calcination temperature above 820°C during catalyst preparation. This promotes Pt sintering with a concomitant decrease in the length of the three-phase-boundary length and in I_0 (*39*). However, this also causes a decrease in catalyst surface area, thus in r_0, so that $r_0/(I_0/2F)$ cannot be increased. Therefore it appears very difficult to obtain larger Λ values for this reaction.

Consequently, although CH_4 oxidation on Pt follows on the same straight line with all reactions studied so far for NEMCA (Figs. 8a and 8b), the low Λ values do not allow one to conclude that the observed dramatic increase in the rate of CO_2 production is due only to NEMCA but suggest that a significant part of the rate enhancement may be due to direct electrocatalysis, i.e., the overall reaction

$$CH_4 + 4O^{2-} \rightarrow CO_2 + 2H_2O + 8e^- \quad (18)$$

In analogy with the currently prevailing ideas on the mechanism of CH_4 activation on metal and metal oxide surfaces (*35*), one would expect the rate-limiting-step (rls) of the electrocatalytic reaction (18) to be

$$CH_4 + O^{2-} \rightarrow CH_3 \cdot (a) + OH(a) + 2e^- \quad (19)$$

where (a) stands for an adsorbed species. One might object to the above scheme in view of the fact that measured τ values are, as in previous NEMCA studies, of the order $2FN/I$ or even longer, whereas electrocatalysis at the geometric tpb would imply negligible τ values during galvanostatic transients. If, however, one postulates that reaction (18) (or 19) takes place not only at the geometric tpb but allover the Pt surface, i.e.,that CH_4 reacts with the spillover ions produced at the tpb (*1–19*) then one can explain the observed magnitude of τ.

Reaction (18) can explain Λ values up to 1 for $I > 0$. In this work Λ values up to 3 were measured, in qualitative agreement with Λ values up to 5 reported in the literature (20). This additional enhancement can then be attributed to NEMCA, i.e., to an enhancement in the overall catalytic reaction

$$CH_4 + 2O_2 \rightarrow CO_2 + 2H_2O, \quad (20)$$

the rls of which, must, by analogy be

$$CH_4 + O(a) \rightarrow CH_3 \cdot (a) + OH(a). \quad (21)$$

Such an enhancement is to be expected, as increasing V_{WR} and $e\Phi$, i.e., $I > 0$, is known to weaken the metal–oxygen chemisorptive bond (*2, 5, 6, 38*) and thus cause electrophobic behaviour (*1, 2, 5*).

The observed very pronounced rate *increase* upon O^{2-} *removal* from the catalyst (i.e., $\Lambda < 0$ for $I < 0$) would, at first glance, be strongly indicative of NEMCA. The fact, however, that Λ is usually close to -1 suggests that the enhancement may be due to an electrocatalytic reaction which generates both CO_2 and O^{2-}. Such an electrocatalytic reaction is

$$CH_4 + 2O(a) + 2e^- \rightarrow CH_3 \cdot (a) + OH(a) + O^{2-}, \quad (22)$$

where adsorbed methyl radicals are subsequently oxidized to CO_2 and H_2O.

It is interesting to note that the sum of the anodic ($I > 0$) half-cell reaction (19) plus the cathodic ($I < 0$) half-cell reaction (22) is twice the rls (Eq. 21) of the *catalytic* reaction (20). On the basis of these observations it is tempting to speculate that even under open-circuit conditions ($I = 0$) the oxidation of CH_4 proceeds via coupling of the two half-cell reactions (19) and (22), i.e., that the catalytic reaction proceeds via a corrosion-

type mechanism. If this were the case then one would measure $\Lambda = 1$ for positive I values and $\Lambda = -1$ for negative I values, in reasonably good agreement with experiment (Fig. 7).

In view of the fact that, as shown by the magnitude of τ, rate changes take place all-over the Pt catalyst surface, one might object to the above mechanism on the basis of the argument that electrocatalytic reactions such as reactions (19), (22), and (8) must take place at the geometric three-phase boundaries. However, recent studies have shown that due to the high mobility of spillover oxide ions but also of chemisorbed oxygen on Pt at elevated temperatures (*40*), the thickness δ of the electrocatalytically active zone can extend hundreds of atomic units on the Pt surface (*39*).

Consequently the task of distinguishing between NEMCA and electrocatalysis at these elevated temperatures, where $2Fr_0/I_0$ is of the order of unity, is not trivial. The NEMCA behaviour of catalytic reactions studied at lower temperatures where $|\Lambda| \approx 2Fr_0/I_0 \gg 1$ has been attributed to a spillover of oxide ions (together with their compensating charge in the metal) originating from the solid electrolyte and spreading over the catalyst surface, altering its work function and catalytic properties. Direct in situ XPS evidence for this on Ag/YSZ at 400°C has been provided by the experiments of Arakawa *et al.* (*41, 42*) who, in addition to an O 1*s* signal corresponding to covalently bonded atomic oxygen, observed the appearance of O 1*s* signal corresponding to ionically bonded oxygen upon polarizing the Ag/YSZ interface. This latter peak appeared only during O^{2-} pumping and disappeared upon current interruption (*41, 42*). The time evolution of this peak parallels the rate evolution upon galvanostatic transients during C_2H_4 expoxidation (*41, 42, 19*).

The current interpretation of NEMCA (*1–19*) assumes that the spillover oxide ions can remain on the catalyst surface long enough to change its chemisorptive properties, acting as promoters. This implies that they are less reactive with the oxidizable reactants than covalently bonded atomic oxygen, i.e., that

$$2FN/I > \tau_{O^{2-}} > \tau_O, \tag{23}$$

where $\tau_{O^{2-}}$ and τ_O stand for the mean residence (reaction) time of O^{2-} and O(a) on the surface; $\tau_{O^{2-}}$ and τ_O are the inverse of the turnover frequency (TOF) of the oxidation reaction involving O^{2-} and O(a), respectively. This is indeed the case in low-temperature NEMCA studies, e.g., C_2H_4 oxidation on Pt (*2, 5*). Thus from Fig. 6 in Ref. (*5*) one estimates $\tau_{O^{2-}}$ to be 360 s from the rate relaxation curve upon current interruption, while τ_O is 0.3 s under open-circuit conditions (TOF = 3.67 s^{-1}) and $\tau_O \approx 0.1$ s (TOF = 95.4 s^{-1}) under maximum NEMCA-induced rate conditions. In the same experiment $2FN/I$ is 760 s, i.e., both inequalities (Eq. 23) are satisfied. This shows conclusively that at these low temperatures (380°C) the spillover oxide ions are indeed less reactive with C_2H_4 than covalently bonded atomic oxygen.

In the present high-temperature study, however, this may not be the case, in view of the fact that O^- and O^{2-} are considered in the literature (*25, 35, 43*) to be ideal reactants for the abstraction of H from CH_4 and for the initiation of the combustion process (reaction (19)). This is also supported by the very fast rate transients upon current interruption (Fig. 6) which indicate that $\tau_{O^{2-}}$ is indeed very short. Consequently in the present study the spillover oxide ions may indeed be the main reactant.

Consequently in order to show that the observed rate enhancement over the entire catalyst surface can indeed be attributed, at least to a large extent, to the electrocatalytic reactions (19) and (22) it remains to be shown that the thickness δ of the electrocatalytically active zone can indeed reach the thickness L of the porous Pt catalyst film ($L \sim 6\ \mu$m). In a recent paper involving solid electrolyte cyclic voltammetry (*39*) it was shown that δ can be estimated, provided one knows the surface diffusivity D_O of atomic

oxygen which has been measured by Lewis and Gomer (*40*). These authors expressed their results as

$$D_0 = \alpha^2 r \exp(\Delta S/R) \exp(-E_0/RT) \quad (24)$$

with $\alpha = 3$ Å, $\Delta S = 17$ cal/(mol K), $r = 10^{12}$ s^{-1}, and $E_0 = 34.1$ kcal/mole.

Although this expression was obtained for relatively low O(a) coverages, it is used routinely for the computation of D_0 on Pt films even at high coverages (*44*). At T = 923 K Eq. (21) gives $D_0 = 3.9 \times 10^{-8}$ $cm^2/s = 3.94$ $\mu m^2/s$. One can then estimate δ from (*39*):

$$\delta \approx (D_O \tau_O)^{1/2}. \quad (23)$$

Since τ_O is typically of the order 1–10 s (e.g., Figs. 3 to 6) in the present work, it follows that δ is of the order of 2 to 6 μm, i.e., it is indeed comparable to the thickness of the catalyst film.

Rate enhancement interpretation. On the basis of the previous discussion one can interpret the observed dramatic rate enhancement in two different ways, one invoking only NEMCA and one invoking both electrocatalysis and NEMCA. Both interpretations can fit the experimental observations, although the latter appears to be the most probable one.

NEMCA interpretation. Oxide ions O^{2-} arriving at the three phase boundaries (for $I > 0$) follow two paths:

$$O^{2-} \rightarrow O(a) + 2e^- \quad (26)$$

$$O^{2-} \rightarrow (O^{\alpha-} - q^{\alpha+}) + 2e^-. \quad (27)$$

Reaction (26) produces adsorbed atomic oxygen O(a) which can diffuse rapidly on the catalyst surface and react with CH_4. Reaction (27) produces spillover oxide ions which spread over the catalyst surface, and increase substantially the catalyst work function, thus weakening the O(a) chemisorptive bond, lowering the activation energy of the catalytic reaction

$$CH_4 + O(a) \rightarrow CH_3 \cdot (a) + OH(a) \quad (21)$$

which is the rls of the CH_4 combustion to CO_2 and thus enhancing the rate of the above reaction.

The explanation then of both the linear E vs $e\Phi$ and of the exponential r vs $e\Phi$ dependence is the same as in the case of C_2H_4 oxidation on Pt and is based on Boudart's correlation (*2*, *38*),

$$\Delta(-\Delta H_0) = -\Delta e\Phi, \quad (28)$$

leading to (*2*)

$$\Delta E = -\Delta e\Phi. \quad (29)$$

The observed linear decrease in activation energy and exponential increase in r with decreasing $e\Phi$ ($I < 0$) can be attributed to the enhancement in the bonding of $CH_3\cdot$ (a) on the catalyst surface with increasing Fermi level (*37*) or, equivalently (*2*), decreasing work function.

A strengthening in the bonding of $CH_3\cdot$ on the catalyst surface which is a product in the rls step (*21*) will cause a decrease in activation energy, as experimentally observed.

Electrocatalytic and NEMCA interpretation. Methane reacts preferentially not with chemisorbed oxygen but with O^{2-} or spillover dipoles ($O^{\alpha-} - q^{\alpha+}$) over a zone extending from the three-phase boundaries allover the Pt surface:

$$CH_4 + O^{2-} \rightarrow CH_3 \cdot (a) + OH(a) + 2e. \quad (19)$$

This accounts for $\Lambda = 1$ ($I > 0$, Fig. 7). Any additional rate enhancement ($\Lambda > 1$) is due to NEMCA and can be explained as previously due to the weakening of the Pt=O bond of O(a) involved in the reaction

$$CH_4 + O(a) \rightarrow CH_3 \cdot (a) + OH(a). \quad (21)$$

Since (19) is an electrocatalytic reaction its rate will be exponentially increasing function of V_{WR} (from the Butler–Vomer equation) and its activation energy will be a linear function of V_{WR} (*45*) in good agreement with experiment (Fig. 9).

When O^{2-} is removed from the catalyst ($I < 0$) then the electrocatalytic reaction

$$CH_4 + 2O(a) + 2e^- \rightarrow O^{2-} + CH_3 \cdot (a) + OH(a) \quad (22)$$

is activated, leading again to the combustion of CH_4. This accounts exactly for $\Lambda = -1$, in excellent agreement with experiment, and also for the linear decrease in E with decreasing V_{WR} and the exponential increase in the rate via the Butler–Volmer equation (*2*, *45*). The very good agreement between this model and experiment strongly corroborates its validity.

On the basis of this interpretation one could speculate that even under open-circuit conditions ($I = 0$) the macroscopically observed catalytic rate results from the coupling of the two electrocatalytic reactions (19) and (22). This corrosion-like interpretation of the catalytic mechanism may not necessarily be restricted to this catalytic system.

SUMMARY

The catalytic activity of Pt films interfaced with YSZ for CH_4 oxidation to CO_2 can be reversibly enhanced by as much as a factor of 70 by polarizing the Pt/YSZ interface. This reaction system represents a limiting case of NEMCA, in that, due to the slow kinetics of CH_4 oxidation and the concomitantly high operating temperature and exchange current I_0, electrocatalytic reactions, in addition to NEMCA, play an important role in the observed kinetic behaviour.

ACKNOWLEDGMENTS

Financial support by the EEC Non-nuclear Energy and JOULE programs is gratefully acknowledged. One of the authors (CGV) also thanks the Alexander von Humboldt Foundation of Germany for a fellowship.

REFERENCES

1. Vayenas, C. G., Bebelis, S., and Ladas, S., Nature (London) **343** (6259), 625 (1990).
2. Vayenas, C. G., Bebelis, S., Yentekakis, I. V., and Lintz, H.-G., *Catal. Today* **11**(3), 303 (1992).
3. Yentekakis, I. V., and Vayenas, C. G., *J. Catal.* **111**, 170 (1988).
4. Vayenas, C. G., Bebelis, S., and Neophytides, S., *J. Phys. Chem.* **92**, 5083 (1988).
5. Bebelis, S., and Vayenas, C. G., *J. Catal.* **118**, 125 (1989).
6. Neophytides, S., and Vayenas, C. G., *J. Catal.* **118**, 147 (1989).
7. Vayenas, C. G., Bebelis, S., Neophytides, S., and Yentekakis, I. V., *Appl. Phys. A* **49**, 95 (1989).
8. Vayenas, C. G., Bebelis, S., Yentekakis, I. V., Tsiakaras, P., and Karasali, H., *Platinum Met. Rev.* **34**(3), 122 (1990).
9. Vayenas, C. G., and Neophytides, S., *J. Catal.* **127**, 645 (1991).
10. Vayenas, C. G., Bebelis, S., and Despotopoulou, M., *J. Catal.* **128**, 415 (1991).
11. Ladas, S., Bebelis, S., and Vayenas, C. G., *Surf. Sci.* **251/252**, 1062 (1991).
12. Lintz, H-G., and Vayenas, C. G., *Angew. Chem.* **101**, 725 (1989); *Angew. Chem. Int. Ed. Engl.* **28**, 708 (1989).
13. Vayenas, C. G., Bebelis, S., and Neophytides, S., *in* "New Developments in Selective Oxidation" (G. Genti and P. Trifiro, Eds.), Studies in Surface Science and Catalysis, Vol. 55, p. 643. Elsevier, Amsterdam, 1990.
14. Vayenas, C. G., Bebelis, S., Yentekakis, I. V., Tsiakaras, P., Karasali, H., and Karavasilis, Ch., *ISSI Lett.* **2**, 5 (1991).
15. Vayenas, C. G., Bebelis, S., and Kyriazis, C., *Chemtech* **21**, 500 (1991).
16. Bebelis, S., Karavasilis, Ch., Karasali, H., Tsiakaras, P., Yentekakis, I. V., and Vayenas, C. G., *in* "Proceedings 2nd International Symposium on Solid Oxide Fuel Cells, Athens, Greece," pp. 353–360. EEC Publ., Luxembourg, 1991.
17. Vayenas, C. G., Bebelis, S., Yentekakis, I. V., Tsiakaras, P., Karasali, H., and Karavasilis, Ch., *in* "Proceedings, 3rd International Symposium on Systems with Fast Ionic Transport, Holzhau, Germany, 1991," *Mater. Sci. Forum* **76**, 141 (1991); Tsiakaras, P., and Vayenas, C. G., p. 179; Karasali, H., and Vayenas, C. G., p. 171; Karavasilis, Ch., Bebelis, S., and Vayenas, C. G., p. 175; Bebelis, S., and Vayenas, C. G., p. 221.
18. Bebelis, S., and Vayenas, C. G., *J. Catal.*, in press.
19. Bebelis, S., and Vayenas, C. G., *J. Catal.*, in press.
20. Eng, D., and Stoukides, M., *J. Catal.* **130**, 306 (1991).
21. Alqahtany, H., Chiang, P., Eng. D., Stoukides, M., and Robbat, A., *Catal. Lett.*, **13**, 289 (1992).
22. Arakawa, T., Saito, A., and Shiokawa, J., *Chem. Phys. Lett.* **94**, 250 (1983).
23. Arakawa, T., Saito, A., and Shiokawa, J., *Appl. Surf. Sci.* **16**, 365 (1983).
24. Schröder, W., and Hölzl, J., *Solid State Commun.* **24**, 777 (1977).
25. Eng, D., and Stoukides, M., *Catal. Rev.-Sci. Eng.* **33**(3&4), 375 (1991).

26. Seimanides, S., Tsiakaras, P., Verykios, X. E., and Vayenas, C. G., *Appl. Catal.* **68,** 41 (1991).
27. Eng, D., and Stoukides, M., *Catal. Lett.* **9,** 47 (1991).
28. Tsiakaras, P., and Vayenas, C. G., *J. Catal.*, submitted.
29. Firth, J. G., and Holland, H. B., *Trans. Faraday Soc.* **65,** 1121 (1969).
30. Yao, Y. F. Y., *Ind. Eng. Chem. Prod. Res. Dev.* **19,** 293 (1980).
31. Trimm, D. L., and Lam, C., *Chem. Eng. Sci.* **35,** 1405 (1980).
32. Cullis, C. F., and Willat, B. M., *J. Catal.* **83,** 267 (1983).
33. Otto, K., *Langmuir* **5,** 1364 (1989).
34. Hicks, R. F., Qi, H., Young, M. L., and Lee, R. G., *J. Catal.* **122,** 280 (1990).
35. Garibyan, T. A., and Margolis, L. Ya, *Catal. Rev.-Sci. Eng.* **31**(4), 355 (1989–90).
36. Minot, C., Van Hove, M. A., and Somorjai, G. A., *Surf. Sci.* **127,** 441 (1982).
37. Zheng, C., Apeloig, Y., and Hoffmann, R., *J. Am. Chem. Soc.* **110,** 749 (1988).
38. Boudart, M., *J. Am. Chem. Soc.* **74,** 3556 (1952).
39. Vayenas, C. G., Ioannides, A., and Bebelis, S., *J. Catal.* **129,** 69 (1991).
40. Lewis, R., and Gomer, R., *Surf. Sci.* **12,** 157 (1980).
41. Arakawa, T., Saito, A., and Shiokawa, J., *Chem. Phys. Lett.* **94,** 250 (1983).
42. Arakawa, T., Saito, A., and Shiokawa, J., *Appl. Surf. Sci.* **16,** 365 (1983).
43. Tong, Y., Rosynek, M. P., and Lunsford, J. H., *J. Catal.* **126,** 291 (1990).
44. Wang, D. Y., and Nowick, A. S., *J. Electrochem. Soc.* **128**(1), 55 (1981).
45. Bockris, J. O'M., and Reddy, A. K. N., "Modern Electrochemistry," Vol. 2. Plenum Press, New York, 1970.